JPE 9-5-10

Small-Signal Modeling and Control of Three-Phase Bridge Boost Rectifiers under Non-Sinusoidal Conditions

Yuan Chang*, Liu Jinjun†, Wang Xiaoyu*, and Wang Zhaoan*

†*School of Electrical Engineering, Xi'an Jiaotong University, Xi'an, China

ABSTRACT

This paper proposes a systematic approach to the modeling of the small-signal characteristics of three-phase bridge boost rectifiers under non-sinusoidal conditions. The main obstacle to the conventional synchronous d-q frame modeling approach is that it is unable to identify a steady-state under non-sinusoidal conditions. However, for most applications under non-sinusoidal conditions, the current loops of boost rectifiers are designed to have a bandwidth that is much higher than typical harmonics frequencies in order to achieve good current control for these harmonic components. Therefore a quasi-static method is applied to the proposed modeling approach. The converter small-signal characteristics developed from conventional synchronous frame modeling under different operating points are investigated and a worst case point is then located for the current loop design. Both qualitative and quantitative analyses are presented. It is observed that operating points influence the converter low frequency characteristics but hardly affect the dominant poles. The relationship between power stage parameters, system poles and zeroes is also presented which offers good support for the system design. Both the simulation and experimental results verified the analysis and proposed modeling approach. Finally, the practical case of a parallel active power filter is studied to present the modeling approach and the resultant regulator design procedure. The system performance further verifies the whole analysis.

Keywords: Small-signal modeling, Boost rectifier, Non-sinusoidal

1. Introduction

Three-phase PWM boost rectifiers are widely employed as front-end power processing units due to their unity power factor and harmonics free features. Control is a key issue for the performance of these rectifiers, and has been a hot research spot ever since the proposal of the three-phase PWM boost rectifier[1-5]. Theoretically, an accurate model of its power stage is the fundament of the design of the whole control system. Power electronic circuits are discrete and nonlinear due to their switching nature. There are some mature methods for obtaining models of certain power electronic circuits. For Dc-Dc converters, a systematic approach based on averaging and linearization has been developed for analyzing system performance and stability [6-8]. For three-phase converters, there are no static operating points due to their sinusoidal utility voltage and input current. As a result, a rotating transformation is applied to get the synchronous-frame model. The rotating transformation can transmit three-phase sinusoidal variables with synchronous

Manuscript received Dec. 14, 2008; revised July 28, 2009
†Corresponding Author: jjliu@mail.xjtu.edu.cn
Tel: +86-29-82667858, Fax: +86-29-82665223, Xi'an Jiaotong University.
*School of Electrical Engineering, Xi'an Jiaotong University

frequencies into constants. Therefore, the system operating points in a synchronous-frame can be found. Then a small-signal model of a three-phase converter which is working in sinusoidal condition is obtained [9-13].

Since the three-phase boost rectifier has matured in both the structure of its power circuits and in its control strategy, it is also applied to other applications such as power quality control. Power quality problems have been drawing more and more attention these years, especially with the development of a modern electronics industry and the continuous proliferation of nonlinear types of electric loads. To solve these problems, passive power filters were used at the beginning, and the active power filter (APF) is now widely researched and has been put into many field installations[14,15]. Parallel active power filters are a popular topology of APF and are commonly based on a three-phase boost rectifier topology [16-20].

In a PAPF application, the AC-side current is not sinusoidal but includes many harmonic components. The non-sinusoidal working condition brings difficulties for the modeling process. Although a rotating transformation is applied, there is still no static operating point in the synchronous-frame coordinates. So currently there is no widely accepted model for the main circuit of a PAPF, which is a critical issue for the application of power quality control.

This paper uses the modeling of a single phase PFC circuit for reference. In the case of a single phase PFC, the quasi-static method is widely used [21-23]. It assumes that for the duration of a fast transient response the circuit is quasi-static with a constant input voltage chosen as a worst-case scenario. Such an approach is used for the designing of a current loop controller for a PFC. In the case of a PAPF, since the current loops are ordinarily designed to have a bandwidth that is much higher than the harmonics frequency; the quasi-static method is also valid. Based on this idea, this paper analyses the frequency characteristics of the power stage of a three-phase boost rectifier under different operating points. The relationship between operating points, system poles and zeroes is illustrated. Also the influence of system parameters on the system characteristics is illustrated in detail. The obtained model offers a practical way to design system parameters and a closed-loop current regulator.

This paper is organized as follows. The conventional small-signal modeling process is shown in section Ⅱ, and then the problem statement and the relevant quasi-static modeling method are given in section III. The influence of the operating points and the system parameters on system characteristics is analyzed qualitatively and quantitatively in section Ⅳ. After that, the effectiveness of the proposed modeling method is illustrated based on simulations and experimental results presented in sections Ⅴ and Ⅵ. Then, section Ⅶ takes a practical PAPF application as an example to present the resultant regulator design procedure. It also provides a further verification for the whole analysis. Finally in section Ⅷ, the conclusions are listed and possible application fields are discussed.

2. Synchronous-Frame Small-Signal Model of Conventional PWM Converter

This section will show a whole small-signal modeling process for a three-phase boost rectifier under sinusoidal conditions. Fig.1 shows the configuration of a three-phase boost rectifier.

Using a switching function to represent the real switch, the switching model of this circuit can be obtained easily. Applying an average operator to the switching model, an average model is derived (Equ.1).

$$\begin{cases} \dfrac{d\bar{\vec{i}}_{l-l}}{dt} = \dfrac{1}{3L}\bar{\vec{v}}_{l-l} - \dfrac{R_{eq}}{L}\bar{\vec{i}}_{l-l} - \dfrac{1}{3L}\vec{d}_{l-l}\bar{v}_{dc} \\ \dfrac{d\bar{v}_{dc}}{dt} = \dfrac{1}{C}\vec{d}_{l-l}^{\,T}\bar{\vec{i}}_{l-l} - \dfrac{\bar{v}_{dc}}{RC} \end{cases} \tag{1}$$

where:

$$\vec{v}_{l-l} = \begin{bmatrix} v_a - v_b \\ v_b - v_c \\ v_c - v_a \end{bmatrix} \quad \vec{i}_{l-l} = \begin{bmatrix} i_a - i_b \\ i_b - i_c \\ i_c - i_a \end{bmatrix} \quad \vec{d}_{l-l} = \begin{bmatrix} d_a - d_b \\ d_b - d_c \\ d_c - d_a \end{bmatrix}$$

and R_{eq} is the series equivalent resistance of L.

As a result of the coordinates transformation, the average model in a synchronous frame is obtained (Equ.2).

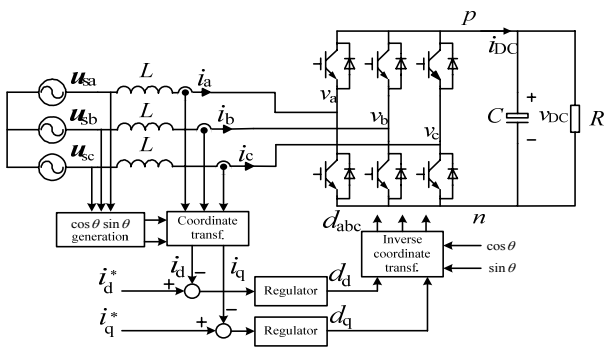

Fig. 1. System configuration of three-phase PWM boost rectifier.

$$\begin{cases} \dfrac{d}{dt}\begin{bmatrix}\bar{i}_d\\ \bar{i}_q\end{bmatrix} = \dfrac{1}{3L}\begin{bmatrix}\bar{v}_d\\ \bar{v}_q\end{bmatrix} - \begin{bmatrix}\dfrac{R_{eq}}{L} & -\omega\\ \omega & \dfrac{R_{eq}}{L}\end{bmatrix}\begin{bmatrix}\bar{i}_d\\ \bar{i}_q\end{bmatrix} - \dfrac{1}{3L}\begin{bmatrix}d_d\\ d_q\end{bmatrix}\bar{v}_{dc} \\ \dfrac{d\bar{v}_{dc}}{dt} = \dfrac{1}{C}\begin{bmatrix}d_d & d_q\end{bmatrix}\begin{bmatrix}\bar{i}_d\\ \bar{i}_q\end{bmatrix} - \dfrac{\bar{v}_{dc}}{RC} \end{cases} \tag{2}$$

Finally, a small-signal model of a boost rectifier around a certain operating point is shown in Equ.(3).

$$\frac{\mathrm{d}}{\mathrm{dt}}\begin{bmatrix}\tilde{i}_d\\ \tilde{i}_q\\ \tilde{v}_{dc}\end{bmatrix} = \begin{bmatrix}\dfrac{R_{eq}}{L} & \omega & -\dfrac{D_d}{3L}\\ -\omega & \dfrac{R_{eq}}{L} & -\dfrac{D_q}{3L}\\ \dfrac{D_d}{C} & \dfrac{D_q}{C} & -\dfrac{1}{RC}\end{bmatrix}\cdot\begin{bmatrix}\tilde{i}_d\\ \tilde{i}_q\\ \tilde{v}_{dc}\end{bmatrix} + \begin{bmatrix}-\dfrac{V_{dc}}{3L} & 0\\ 0 & -\dfrac{V_{dc}}{3L}\\ \dfrac{I_d}{C} & \dfrac{I_q}{C}\end{bmatrix}\cdot\begin{bmatrix}\tilde{d}_d\\ \tilde{d}_q\end{bmatrix} \tag{3}$$

The capital variables (except R_{eq},L,R and C) represent the steady-state operating points.

The control-to-output transfer functions can be derived from system state space equations (Equ.(3)) (the influence of the equivalent resistor on the input inductor is ignored):

$$\frac{i_d(s)}{d_d(s)} = -\frac{V_{dc}}{3L}\frac{s^2 + \left(\dfrac{I_d D_d}{V_{dc}C} + \dfrac{1}{CR}\right)s + \dfrac{I_d D_q \omega}{V_{dc}C} + \dfrac{D_q^{\,2}}{3LC}}{s^3 + \dfrac{s^2}{RC} + \left(\omega^2 + \dfrac{D_d^{\,2}}{3LC} + \dfrac{D_q^{\,2}}{3LC}\right)s + \dfrac{\omega^2}{RC}} \tag{4}$$

$$\frac{i_q(s)}{d_q(s)} = -\frac{V_{dc}}{3L}\frac{s^2 + \left(\dfrac{I_q D_q}{V_{dc}C} + \dfrac{1}{CR}\right)s - \dfrac{I_q D_d \omega}{V_{dc}C} + \dfrac{D_d^{\,2}}{3LC}}{s^3 + \dfrac{s^2}{RC} + \omega^2 s + \dfrac{D_d^{\,2}s}{3LC} + \dfrac{D_q^{\,2}s}{3LC} + \dfrac{\omega^2}{RC}} \tag{5}$$

Due to the mature application of decoupled control, the cross–coupling effect is not discussed in this paper.

The control-to-output transfer functions are used for the design of the current regulators and the whole design procedure is based on a certain static operating point.

3. Problem Statement and Relevant Quasi-Static Modeling Method

The power stage of a PAPF is identical to a three-phase boost rectifier, but i_d and i_q are varying. It's impossible to find a steady-state operating point for a PAPF even in a synchronous frame. For instance, assume the PAPF output current consists of 5th and 7th harmonics, Fig.2 illustrates the waveforms in stationary *abc* coordinates, *αβ* coordinates and synchronous coordinates. It can be easily found that the system states are always fluctuating in a synchronous frame and that no static operating point can be obtained. As a result the aforementioned small signal modeling approach does not work any more. Currently, there is no widely accepted modeling approach for a three-phase boost rectifier under non-sinusoidal conditions and it's becoming a critical issue for many applications like APFs.

The widely used quasi-static modeling method could be used to deal with this problem. Since the current loops of a PAPF are ordinarily designed to have a bandwidth that is much higher than the harmonics frequency, the quasi-static method is also valid. The main steps of the quasi-static modeling method are shown as follows:

1) Obtain a linearized model at different operating points.
2) Compare the resultant linear models, and then choose the worst-case scenario.
   Design a regulator based on the chosen model.
3) Note that when i_d and i_q are varying, the duty ratios d_d and d_q are also varying. The relationship between input current and duty ratio is shown below:

$$D_d = (V_d + 3\omega L I_q - 3R_{eq} I_d)/V_{dc} \tag{6}$$

$$D_q = (V_q - 3\omega L I_d - 3R_{eq} I_q)/V_{dc} \tag{7}$$

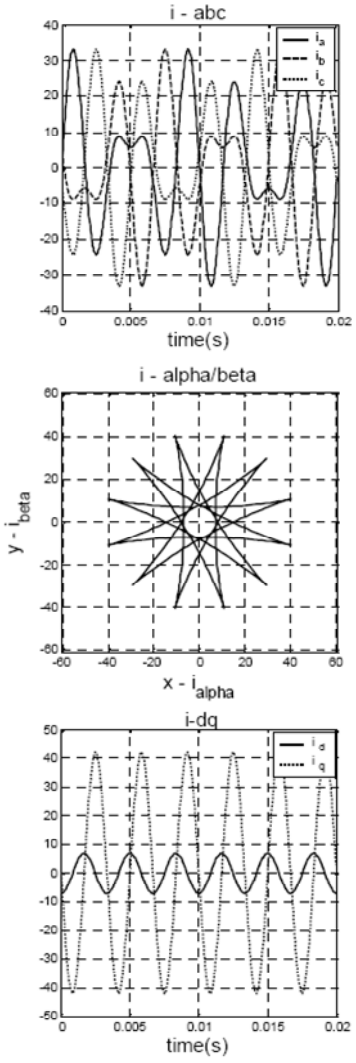

Fig. 2. Illustration of waveforms in stationary coordinates and synchronous coordinates when the time domain waveforms are distorted.

4. Influence of The Operating Points And System Parameters On System Characteristics

This section presents a detailed analysis of the influence of operating points and system parameters on system characteristics. At first, a qualitative analysis is given. According to the system state space equation (Equ.(3)), the control to output transfer functions are obtained. Then the system poles and zeroes can be solved. Since the analytical solutions are too complex, the relationship between roots and coefficients is used for analysis. Through reasonable approximation, the analytical equations will help us to understand the relationship between the system characteristics and the operating points. Then, substituting reasonable system parameters into the obtained transfer functions, pole-zero maps are presented. Furthermore, the influence of the operating points and system parameters on the position of the poles and zeroes is illustrated. After that, bode plots are given showing the system characteristics at different operating points.

A. Formular description.

A detailed analysis of the control-to-output transfer functions (Equ(4)(5)) will offer some helpful information. Theoretically, the dd-to-id transfer function has two zeroes and three poles. One pole and two zeroes are located in comparatively low frequency, and the other two poles are a pair of conjugated poles which dominate the system characteristics. The dq-to-iq transfer function has the same poles as the dd-to-id transfer function, but different zeroes. The detailed analysis is shown below:

Solving the zeroes:

$$0 = s^2 + \left(\frac{I_d D_d}{V_{dc} C} + \frac{1}{CR}\right) s + \frac{I_d D_q \omega}{V_{dc} C} + \frac{D_q^{\,2}}{3LC} \tag{8}$$

$$\begin{cases} z_1 \approx 0 \\ z_2 \approx -\dfrac{1}{C}\left(\dfrac{I_d D_d}{V_{dc}} + \dfrac{1}{R}\right) \end{cases} \tag{9}$$

Solving the poles:

$$0 = s^3 + \frac{s^2}{RC} + \left(\omega^2 + \frac{D_d^{\,2}}{3LC} + \frac{D_q^{\,2}}{3LC}\right) s + \frac{\omega^2}{RC} \tag{10}$$

$$p_1 = c \quad p_2 = a - bi \quad p_3 = a + bi$$

$$\text{when } a^2 + b^2 \gg \omega \;\; 2a \approx -\frac{1}{RC} \;\; c \approx 0 \rightarrow b \gg a$$

$$\rightarrow b^2 \approx \omega^2 + \frac{D_d^{\,2}}{3LC} + \frac{D_q^{\,2}}{3LC} \tag{11}$$

Since the d_q-to-i_q transfer function has the same poles as the d_d-to-i_d transfer function, we just need to solve the zeroes:

$$z_3 = e - fi \quad z_4 = e + fi$$

$$\begin{cases} 2e = -\dfrac{1}{C}\left(\dfrac{I_q D_q}{V_{dc}} + \dfrac{1}{R}\right) \\ f^2 \approx \dfrac{D_d}{C}\left(\dfrac{D_d}{3L} - \dfrac{I_q \omega}{V_{dc}}\right) \end{cases} \tag{12}$$

From Equ. (9), we can deduce that I_d affects Z_2, and that I_q influences Z_3 and Z_4.

Substituting reasonable system parameters (Tab. 1) into Equ. (11)(12), we found that the influence of the operating points on the system poles is negligible. A detailed illustration will be given in the following parts.

B. Poles and zeroes.

Using equations (4)(5)(6)(7) and power stage parameters (Tab. 1), we can get the system control-to-output transfer functions for different operating points. The pole-zero maps are shown in Fig.3.

Table 1. Three-phase boost rectifier power stage parameters.

Utility line to line voltage($V_{s\ l\text{-}l}$)	380 V
DC link capacitor (C)	3300 μF
Load resistor (R)	100 Ω
Input inductor (L)	7.4 mH
Equivalent resistor of L (R_{eq})	0.1 Ω
DC link voltage (V_{dc})	750 V
Switching frequency (f_s)	20 kHz

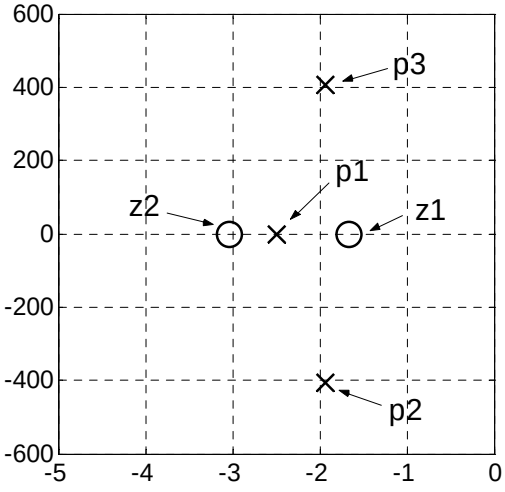

(a) i_d/d_d

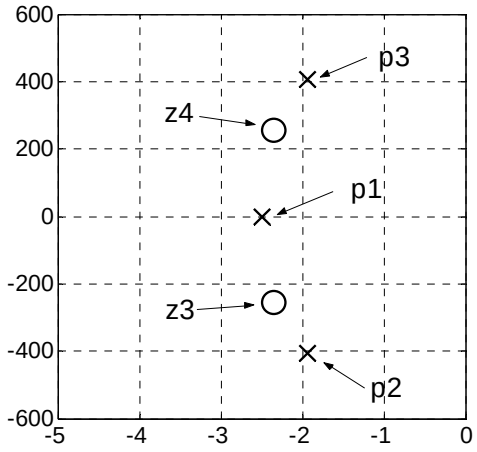

(b) i_q/d_q

Fig. 3. System pole-zero maps.

Then, the relationship between the position of those poles and zeroes and the operating points is illustrated as follows:

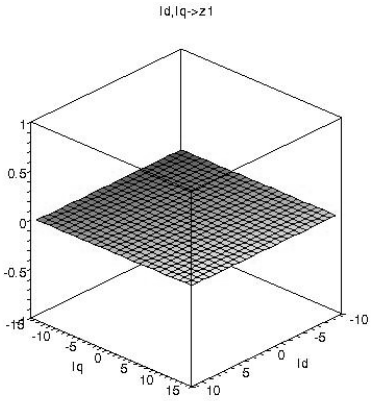

(a) Z_1 versus I_d and I_q

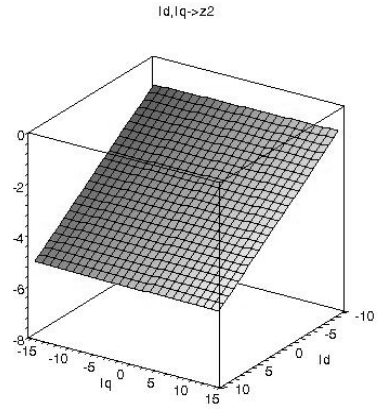

(b) Z_2 versus I_d and I_q

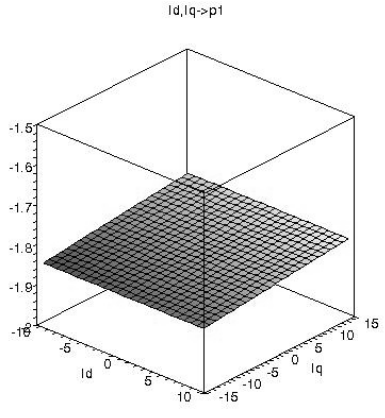

(c) p_1 versus I_d and I_q

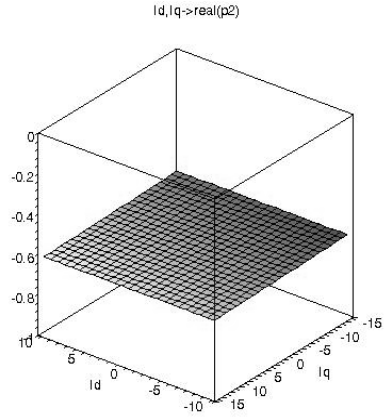

(d) Real part of p_2 versus I_d and I_q

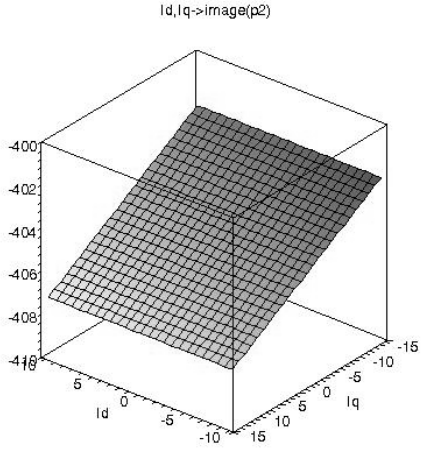

(e) Imaginary part of p_2 versus I_d and I_q

We can deduce from the previous analysis, that I_d affects Z_2, and that I_q influences Z_3 and Z_4, and that the influence of operating points on the system poles is negligible.

Furthermore, the relationship between the poles, the zeroes and the system parameters (AC side inductance (L) and DC side capacitance(C)) are illustrated as follows:

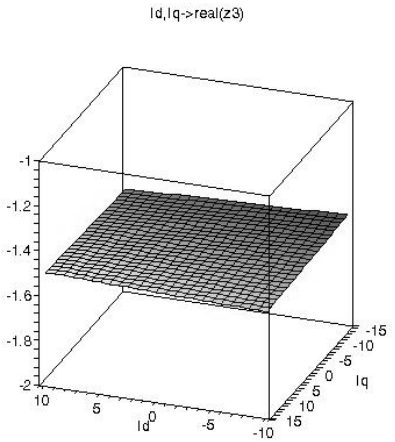

(f) Real part of Z_3 versus I_d and I_q

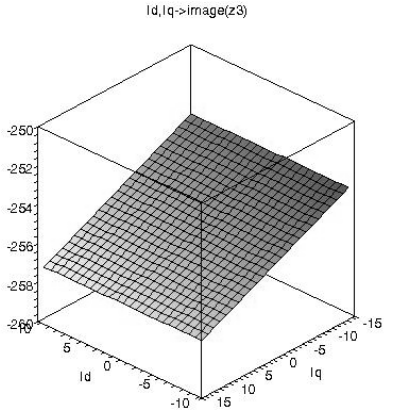

(g) Imaginary part of Z_3 versus I_d and I_q

Fig. 4. Influence of operating points on the system poles and zeroes.

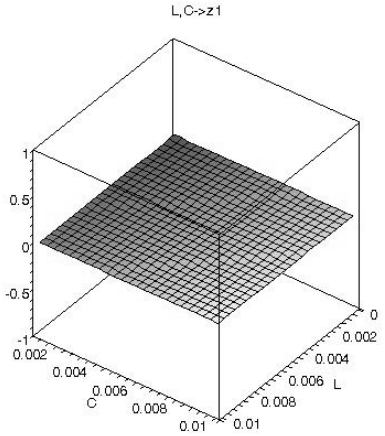

(a) Z_1 versus L and C

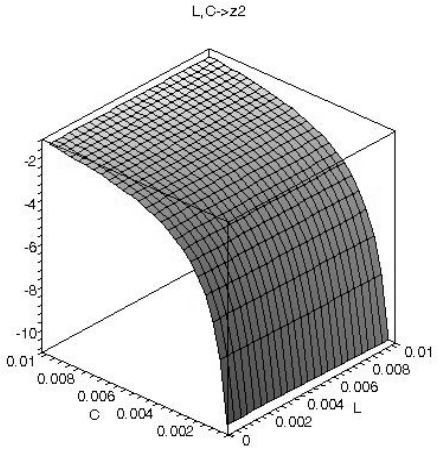

(b) Z_2 versus L and C

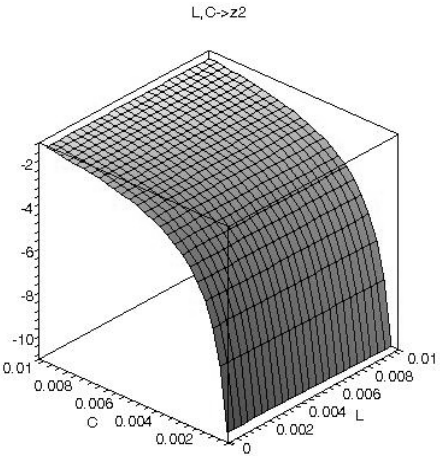

(c) p_1 versus L and C

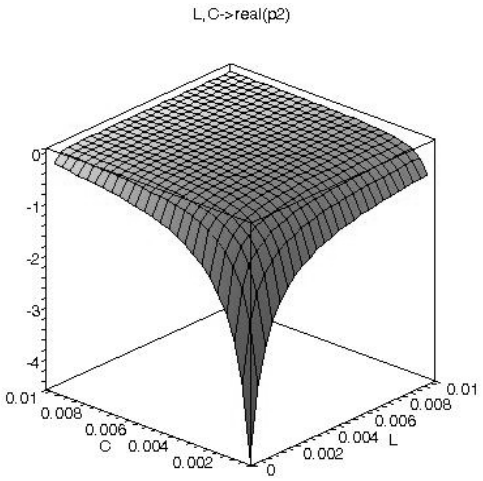

(d) Real part of p_2 versus L and C

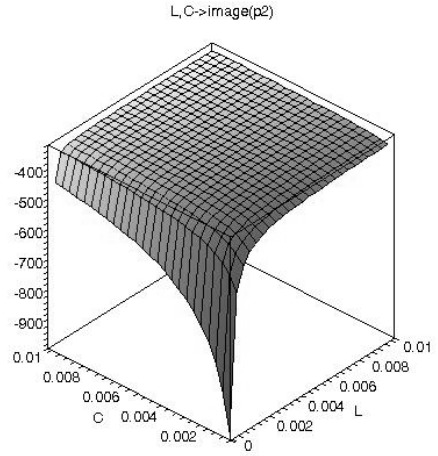

(e) Imaginary part of p_2 versus L and C

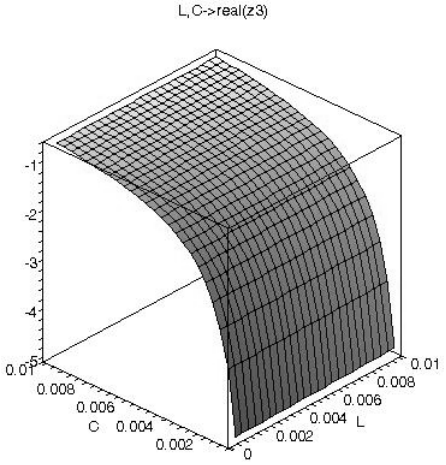

(f) Real part of Z_3 versus L and C

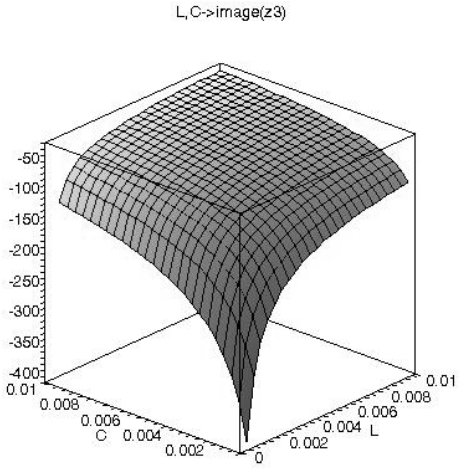

(g) Imaginary part of Z_3 versus L and C

Fig. 5. Influence of operating points on the system poles and zeroes.

The two discussed parameters (L,C) influence the system characteristics greatly. The obtained figures offer good support for the system design.

C. Bode plot.

Fig. 6 shows a comparison of system transfer functions when I_d varies (the selected operating points are shown in Tab. 2). Fig. 7 shows a comparison of system transfer functions when I_q varies (the selected operating points are shown in Tab. 3).

The bode plots accord with the previous analysis. After conducting both the qualitative and the quantitative analysis, important conclusions can be obtained: I_d affects Z_2, I_q influences Z_3 and Z_4, and the influence of the operating points on the system poles is negligible. This conclusion offers a theoretical fundament for the design of a closed-loop current regulator even under non-sinusoidal conditions.

Table 2. Selected operating points when I_d is varying.

Number	I_d(A)	I_q(A)
1	6	0
2	8	0
3	10	0
4	12	0
5	14	0

Table 3. Selected operating points when I_q is varying.

Number	I_d(A)	I_q(A)
1	10	-3
2	10	-6
3	10	0
4	10	3
5	10	6

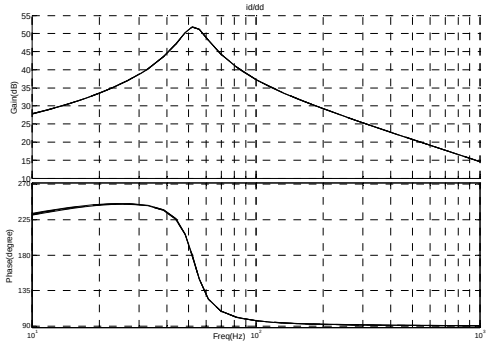

(a) Bode plot of i_d/d_d for different operating points

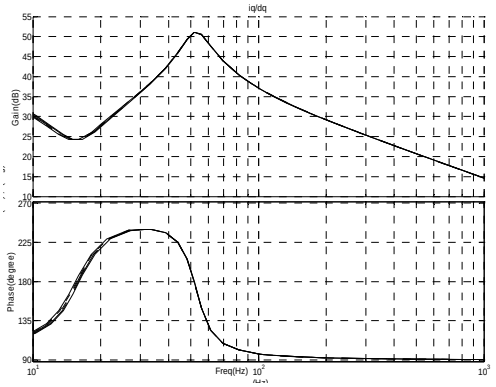

(b) Bode plot of i_q/d_q for different operating points

Fig. 6. Comparison of control-to-output transfer functions when I_d is varying.

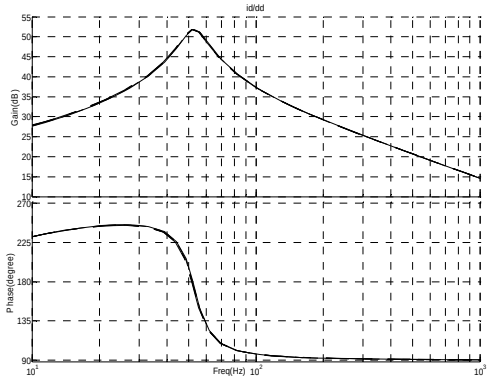

(a) Bode plot of i_d/d_d

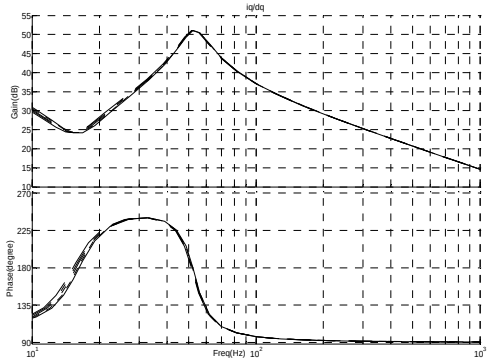

(b) Bode plot of iq/dq

Fig. 7. Comparison of control-to-output transfer functions when I_q is varying.

5. Simulation

Based on the configuration of the boost rectifier shown in Fig.2, a simulation system is built. Fig.8 shows the

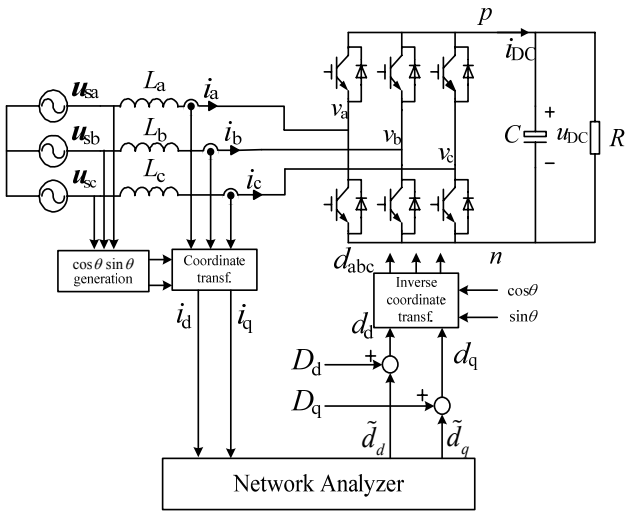

Fig. 8. Open-loop system under test.

open-loop system under test.

Fig.9 shows the corresponding simulation results.

The simulation results verified the theoretical analysis (Fig.(6)(7)).

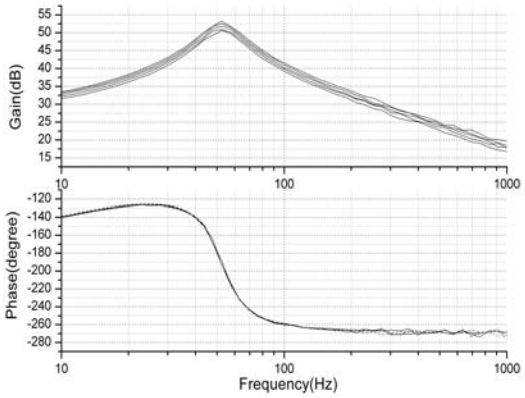

(a) Bode plot of i_d/d_d when I_d is varying

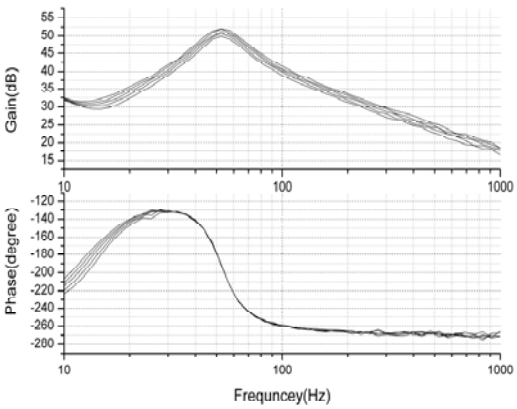

(b) Bode plot of iq/dq when Id is varying

6. Experimental Verification

A 30kW experimental prototype was constructed as shown in Fig.8. The main circuit parameters are shown in Tab.1. The control system employs a DSP (TMS320F2812) and its on-chip A/D and D/A converters. An Agilent® Netwrok/Spectrum/Impedance Analyzer 4395A is used to get the system open-loop characteristics. This section presents the detailed test bench setup, the test steps and the test results.

A. Test bench setup and test steps.

The power stage parameters are shown in Tab. 1, and the notable settings for the network analyzer are shown below:

1) Sweep frequency range. Since the lower limit frequency of the network analyzer is 10Hz, the frequency range is selected from 10Hz to 1000Hz.
2) Input filter bandwidth (IF BW). The IF bandwidth

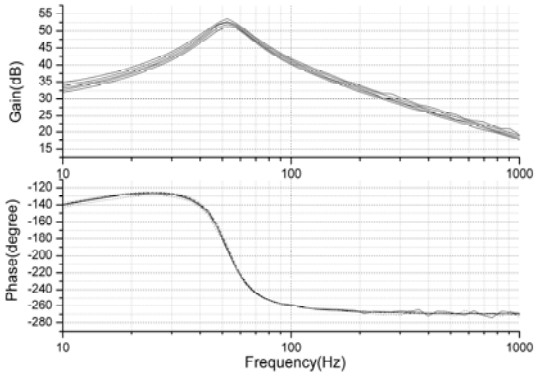

(c) Bode plot of id/dd when Iq is varying

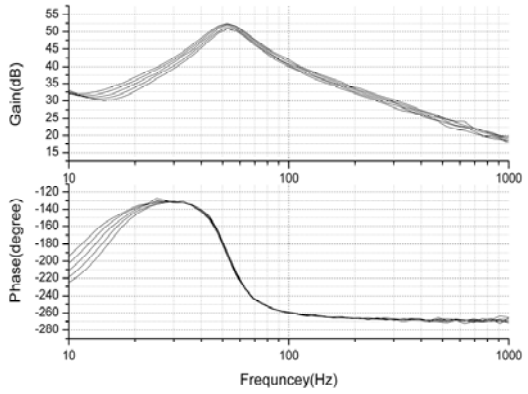

(d) Bode plot of iq/dq when Iq is varying

Fig. 9. Simulation results.

measurement frequency, so, the IF bandwidth in should be set to be equal to or less than 1/5 of the this test is set to 2 Hz.

3) Averaging. Averaging computes each data point based on an exponential average of consecutive sweeps. A high averaging factor gives the best signal-to-noise ratio, but slows the trace update time. In this case, the averaging factor is selected to be 2.

4) Delay compensation. The A/D and D/A conversions bring time delays to the measurements. The network analyzer offers a delay compensation function. Since the sampling rate of the A/D and D/A conversions is 20kHz, the compensated time is set to 100μs.

The main test steps are shown below:

1) Soft-start for safety.
2) Move the operating point to the expected value gradually.

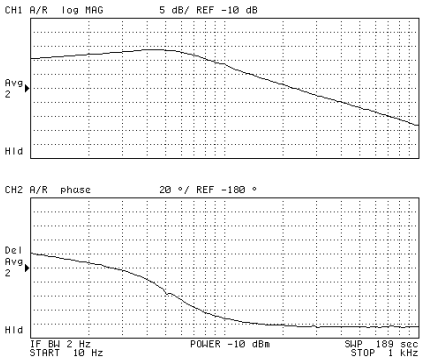

(a) Bode plot of i_d/d_d

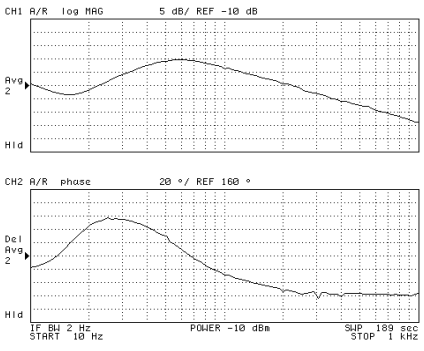

(b) Bode plot of i_q/d_q

Fig. 10. Measured control-to-current bode plots.

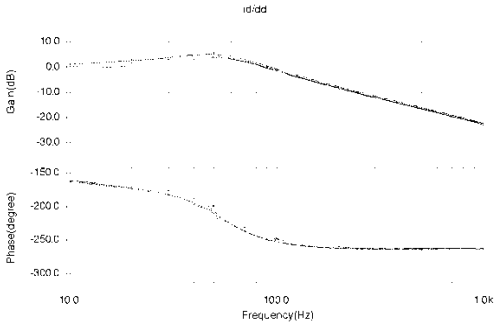

(a) Bode plot of i_d/d_d when I_d is varying

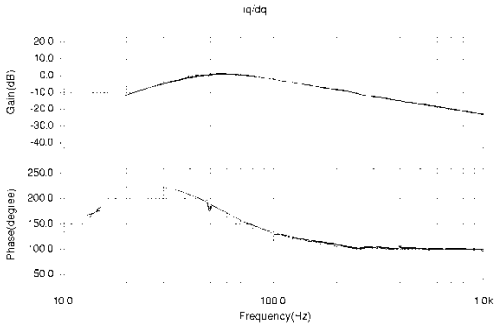

(b) Bode plot of i_q/d_q when I_d is varying

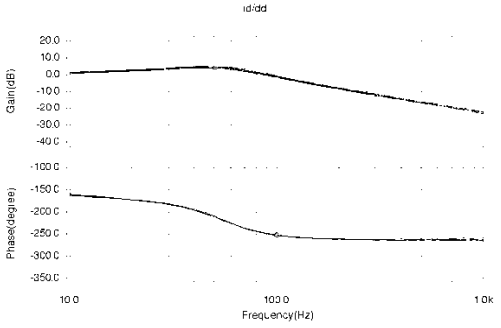

(c) Bode plot of i_d/d_d when I_q is varying

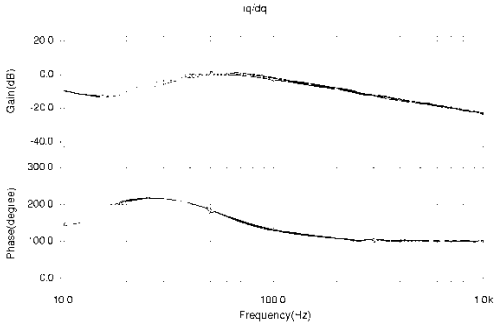

(d) Bode plot of i_q/d_q when I_q is varying

Fig. 11. Experimental results.

3) Cut off the control close-loop and start the measurement.

B. Test Results.

One set of system control-to-output transfer functions is shown in the form of a bode plot (Fig.10). It should be noted that i_d/d_d and i_q/d_q are scaled due to the measurements, as well as the A/D and D/A processes. The scale coefficient is 30, so the gain curves should be shifted about 30dB.

Fig.11 redraws all the measured data for comparison.

7. Regulator Design Procedure

Following the previous analysis, this section discusses the resultant design process, and a practical PAPF case is used as an instance.

For the *d* channel current regulator, since I_d influences the system's low frequency characteristics – a higher I_d leads to a lower low frequency d_d-to-i_d gain, the operating point with the highest I_d should be selected as the worst-case scenario (Fig.4(b)). For the *q* channel current regulator, since I_q influences the system's low frequency characteristics – a higher I_q leads to a lower low frequency d_q-to-i_q gain, the operating point with highest I_q should be selected as the worst-case scenario (Fig.4(g)). Then the regulator design procedure can be obtained:

1) Find the operating point with highest I_d.
2) Design the *d* channel current regulator based on a linearized model at the selected operating point.
3) Find out the operating point with highest I_q.
4) Design the *q* channel current regulator based on a linearized model at the selected operating point.

The experimental prototype is used as a parallel active power filter. The harmonics source is a three-phase uncontrolled rectifier with an inductive load. Fig.12 shows the configuration of the system with a parallel active power filter. The measured load current is shown in Fig. 13.

The harmonics of the load current can be abstracted through the analysis, and the corresponding highest I_d and I_q can be obtained. In this case, the highest I_d is 1.3A, and the highest I_q is 14.4A. Then a system model at the selected operating points can be obtained (Fig.14).

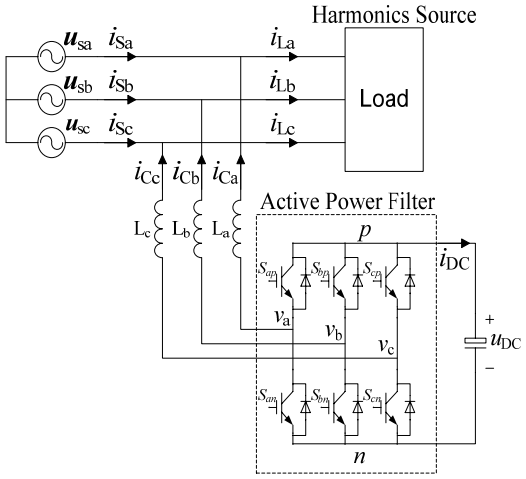

Fig. 12. Configuration of the system with parallel active power filter.

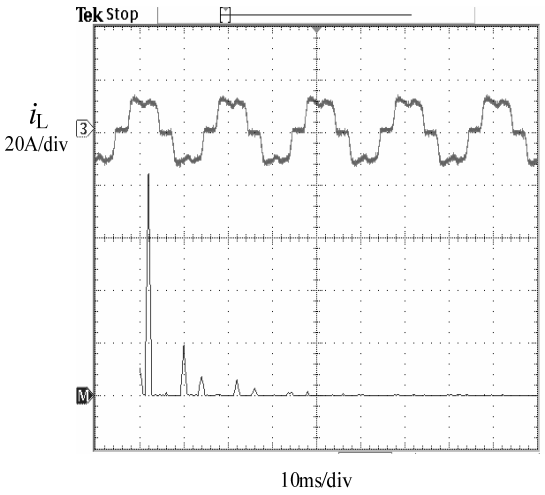

Fig. 13. Waveform and spectrum of load current.

Based on the obtained system bode plots, the current regulator can be designed. In this case, a simple proportional regulator (G_{cd}=-5) is designed for the *d* channel current loop, and another proportional regulator (G_{cq}=-10) is designed for the *q* channel. Fig.15 shows the obtained closed-loop transfer function. Fig.16 shows the compensation performance of a PAPF employing the designed regulator. Fig.17 shows the dynamic performance of a PAPF employing the designed regulator.

The satisfactory static compensation performance and dynamics validate the regulator and further verifies the proposed model.

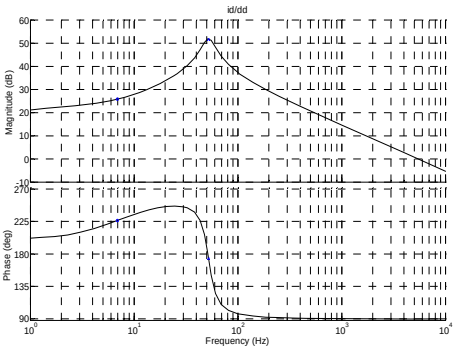

(a) Bode plot of i_d/d_d when I_d equals -3.5

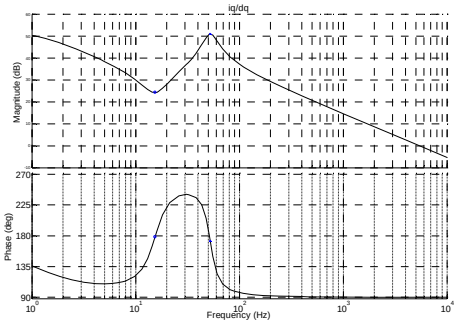

(b) Bode plot of i_q/d_q when I_q equals -14.4

Fig. 14. System characteristics at selected operating points.

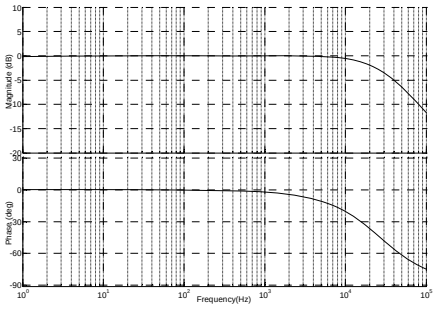

(a) *d* channel

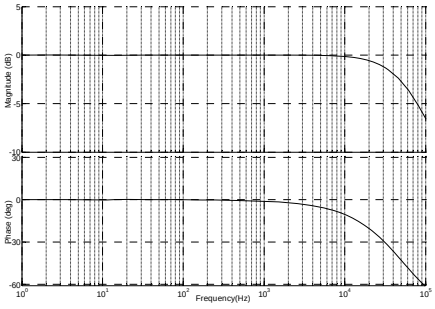

(b) *q* channel

Fig.15. Closed-loop current regulation.

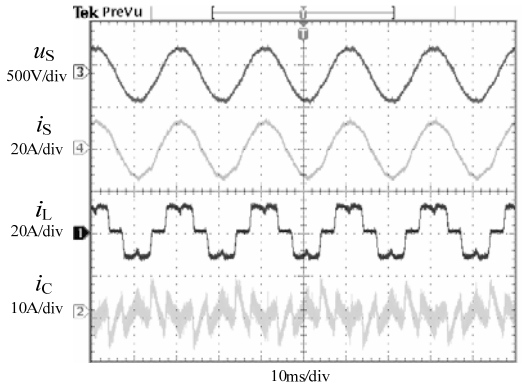

Fig. 16. Compensation performance of PAPF employing the designed regulator.

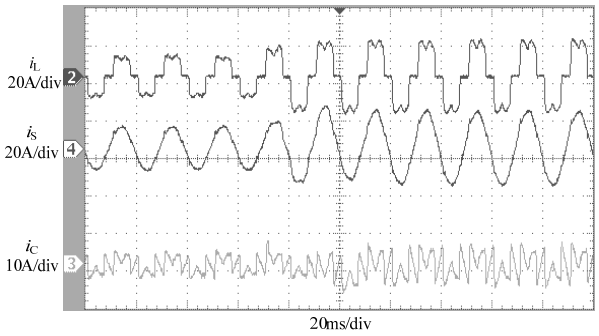

(a) Step up in the load current

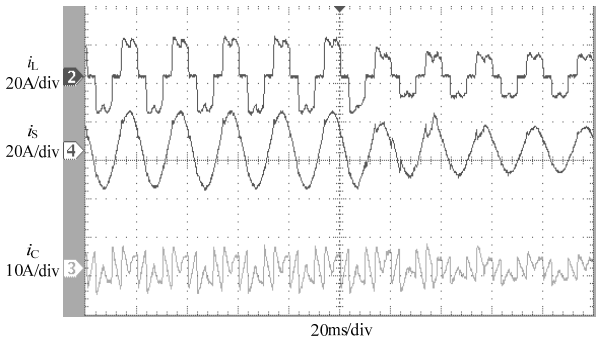

(b) Step down in the load current

Fig. 17. Dynamical performance of PAPF employing the designed regulator.

8. Conclusions

After reviewing a conventional synchronous-frame modeling approach for three-phase boost rectifiers, the main difficulty for the conventional approach is revealed to be an inability to identify a steady-state under non-sinusoidal conditions. Since the current loops of boost

rectifiers are ordinarily designed to have a bandwidth that is much higher than the typical harmonics frequency, this paper applied a quasi-static method for the modeling of a three-phase boost rectifier under non-sinusoidal conditions. The system frequency characteristics under different operating points are studied in detail. After detailed analysis on the system transfer function, this paper found that the variational operating points influence the system's low frequency characteristics but have almost no affect on the dominant poles. Both the simulation and the experimental results verified the analysis and the proposed model.

In summary, the following conclusions can be drawn:

1) For most applications under non-sinusoidal conditions, the current loops of boost rectifiers are usually designed to have a bandwidth that is much higher than the typical harmonics frequency in order to achieve good current control of these harmonic components. So the quasi-static method could be applied to the proposed modeling approach.
2) The system frequency characteristics under different operating points influence the converter low frequency characteristics but hardly affect the dominant poles. This conclusion offers a theoretical fundament for the design of current regulators.
3) The influence of the power stage parameters on the system characteristics is illustrated which strongly supports the system design.
4) From the presented model, the circuit parameters and the current regulator of a closed-lop control can be properly designed.
5) The theoretical results were verified by simulation and experimental results.
6) The resultant design procedure is presented and the system performance further verifies the whole modeling method.

Besides the PAPF case discussed in this paper, there are still many applications that could take advantage of the obtained conclusions. In industrial applications, the operating point of a STATCOM varies depending on the different reactive power commands. And for widely researched distributed generation systems, the converter's operating point is always changing due to volatile input active power. Furthermore, this analysis can be directly extended to the study of unbalanced systems.

References

[1] A.W.Green, J.T.Boys, G.F.Gates. "3-phase voltage sourced reversible rectifier," *IEE proceedings 1988*, 6 (B5): 362-370. 1998.

[2] R.Wu, S.B.Dewan, G.R.Slemon, "Analysis of an ac-to-dc voltage source converter using PWM with phase and amplitude control," *IEEE Trans. Ind. Appl.*, Vol. 27, pp. 355-364, 1991.

[3] Y.Jiang, H.Mao, F.C.Lee, and D.Borojevic, "Simple high performance three-phase boost rectifiers," *IEEE PESC'94*, Rec., Vol. 2, pp. 1158-1164, 1994.

[4] S.Hiti and D.Borojevic, "Control of front-end three-phase three-phase boost rectifier," *in Proc. APEC'94*, pp.927-933, 1994.

[5] S.Hiti et al., "Average curent control of three-phase PWM boost rectifier," *in Proc.PESC'95*, pp.131-137, 1995.

[6] G. W. Wester and R. D. Middlebrook, "Low-Frequency Characterization of Switched dc-dc Converters," *Aerospace and Electronic Systems, IEEE Transactions on*, vol. AES-9, no. 3, pp. 376-385, 1973.

[7] R. D. Middlebrook and S. Cuk, "A general unified approach to modeling switching converter stages," *in IEEE Power Electronics Specialists Conf. Rec.*, pp.18-34, 1976.

[8] V. Vorperian, "Simplify PWM converter analysis using a PWM switch model," Power conversion & Intelligent Motion, Vol. 16, no. 3, pp. 8-11, 1990.

[9] V. Vorperian, R. Tymerski, and F. C. Y. Lee, "Equivalent circuit models for resonant and PWM switches," *IEEE Transactions on Power Electronics*, pp. 205-214, 1989.

[10] C. T. Rim, D. Y. Hu, and G. H. Cho, "Transformers as equivalent circuits for switches: General proofs and D-Q transformation-based analyses," *IEEE Transactions on Industry Applications*, vol. 26, no. 4, pp. 777-785, 1990.

[11] S. Hiti, D. Boroyevich, and C. Cuadros, "Small-signal modeling and control of three-phase PWM converters," in Industry Applications Society Annual Meeting, *Conference Record of the 1994 IEEE*, pp. 1143-1150, 1994.

[12] M. Hengchun, D. Boroyevich, and F. C. Y. Lee, "Novel reduced-order small-signal model of a three-phase PWM rectifier and its application in control design and system analysis," Power Electronics, *IEEE Transactions on*, vol.

13, no. 3, pp. 511-521, 1998.

[13] Y. Yang, M. Kazerani, and V. H. Quintana, "Modeling, control and implementation of three-phase PWM converters," Power Electronics, *IEEE Transactions on*, vol. 18, no. 3, pp. 857-864, 2003.

[14] Akagi, H., "New trends in active filters for power conditioning," Industry Applications, *IEEE Transactions on* , vol.32, no.6pp.1312-1322, Nov/Dec 1996.

[15] Akagi, H., "Active harmonic filters," *Proceedings of the IEEE* , vol.93, no.12pp. 2128- 2141, Dec. 2005.

[16] P. Jintakosonwit, H. Fujita, and H. Akagi, "Control and performance of a fully-digital-controlled shunt active filter for installation on a power distribution system," *IEEE Transactions on Power Electronics*, vol. 17, no. 1, Jan, pp.132-140., 2002.

[17] Wu, J.-C., Jou, H.-L., "Simplified control method for the single-phase active power filter," *Electric Power Applications, IEE Proceedings-* , vol.143, no.3pp.219-224, May 1996.

[18] Casadei, D., Grandi, G., Reggiani, U., Rossi, C., "Control methods for active power filters with minimum measurement requirements," *Applied Power Electronics Conference and Exposition, 1999. APEC '99. Fourteenth Annual* , vol.2, no.pp.1153-1158 vol.2, 14-18, Mar 1999.

[19] K. Chatterjee, B. G. Fernandes, and G. K. Dubey. "An instantaneous reactive volt-ampere compensator and harmonic suppressor system," *Power Electronics, IEEE Transactions on*, 14 (2):381-392, 1999.

[20] S. K. Jain, P. Agarwal, and H. O. Gupta. "A control algorithm for compensation of customer-generated harmonics and reactive power," *Power Delivery, IEEE Transactions on*, 19 (1):357-366, 2004.

[21] Uan-Zo-li, A., Lee, F.C., Noon, J.P, "Modeling and control of single-stage voltage-source and current-source PFC converters," *Applied Power Electronics Conference and Exposition, 2004. APEC '04. Nineteenth Annual IEEE,Volume 3*, Page(s):1778 - 1783 Vol.3, 2004.

[22] Byungcho Choi, Sung-Soo Hong, Hyokil Park, "Modeling and small-signal analysis of controlled on-time boost power-factor-correction circuit," *Industrial Electronics, IEEE Transactions on*, Vol. 48, Issue 1, Page(s):136 – 142 , Feb 2001.

[23] Jian Sun, "Input impedance analysis of single-phase PFC converters," Power Electronics, *IEEE Transactions on*, Vol 20, Issue 2, Page(s):308 – 314, Mar 2005.

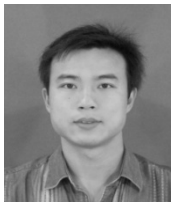

Yuan Chang was born in Hunan, China, in 1981. He received his B.S. degree in electrical engineering from Xi'an Jiaotong University, Xi'an, Shaanxi, in 2003. He is currently working towards his Ph.D. at Xi'an Jiaotong University. His research interests are in the area of power electronics applied to power quality.

Liu Jinjun was born in Hunan province, China in 1970. He received his B.S. and Ph.D. from Xi'an Jiaotong University (XJTU), China in 1992 and 1997 respectively. In 1998, he led the founding of the XJTU/Rockwell Automation Laboratory. From December 1999 until February 2002, he was with the Center for Power Electronics Systems at Virginia Polytechnic Institute and State University, USA, as a Postdoctoral Research Scholar. He then came back to XJTU and in August of 2002 was promoted to Full Professor and head of the Power Electronics and Renewable Energy Center at XJTU. Now he is also serving as an Associate Dean of the School of Electrical Engineering at XJTU. He coauthored 3 books, published over 100 technical papers, and received several provincial and ministerial awards for scientific and career achievements. In 2006 he received the Delta Scholar Award. His research interests are power quality control, renewable energy generation and utility applications of power electronics, and modeling and control of power electronic systems. Dr. Liu has served as the IEEE Power Electronics Society Region 10 Liaison for 3 years. He was actively involved in the organization of several power electronic international conferences, including PESC, APEC and IPEC in Japan, ICPE in Korea, and IPEMC in China, as a committee member or co-chair, or as session chair.

Wang Xiaoyu was born in Shaanxi province, China in 1979. He received his B.S., M.S. and Ph.D. from Xi'an Jiaotong University, China in 2001, 2004 and 2007 respectively, all in Electrical Engineering. He is currently a Lead Engineer employed by GE (China) Research and Development Center Corporation Limited located in Shanghai, China. His research interests are power quality control, and wind energy.

Wang Zhaoan was born in Shanxi province, China in 1945. He received his B.S. and M.S. degrees in electrical engineering from Xi'an Jiaotong University, Xi'an, China, in 1970 and 1982, respectively, and his Ph.D. in electrical engineering from Osaka University, Osaka, Japan, in 1989. From 1970 to 1979, he was a Researcher at the Xi'an Power Rectifier Factory and in 1982 he became a Teacher at Xi'an Jiaotong University. In 1989, he came back to Xi'an Jiaotong University from Japan and has been engaged in teaching and researching in the areas of power electronics and industrial automation ever since. His research interests include power conversion systems, harmonics suppression and reactive power compensation, active power filters, power electronic integration, and packaging technologies.